High Power Laser Science and Engineering, (2024), Vol. 12, e75, 6 pages.
doi:10.1017/hpl.2024.46

HIGH POWER LASER SCIENCE AND ENGINEERING

RESEARCH ARTICLE

High-energy, high-peak-power, sub-nanosecond, spatial super-Gaussian 177 nm vacuum ultraviolet laser

Ning Wen[1,5], Tian-Hao Lv[1,5], Nan Zong[1,2,4], Hong-Wei Gao[1,2,4], Yong Bo[1,2,4], Qin-Jun Peng[1,2,4], Da-Fu Cui[1,2], Zu-Yan Xu[1,2], Xiao-Yang Wang[2], Li-Juan Liu[2], Ru-Kang Li[2], Nan Wang[3], and Xue-Chun Lin[3]

[1] *Key Laboratory of Solid-State Laser, Technical Institute of Physics and Chemistry, Chinese Academy of Sciences, Beijing, China*

[2] *Key Laboratory of Functional Crystal and Laser Technology, Technical Institute of Physics and Chemistry, Chinese Academy of Sciences, Beijing, China*

[3] *Laboratory of All-Solid-State Light Source, Institute of Semiconductors, Chinese Academy of Sciences, Beijing, China*

[4] *Institute of Optical Physics and Engineering Technology, Qilu Zhongke, Jinan, China*

[5] *University of Chinese Academy of Sciences, Beijing, China*

(Received 28 April 2024; revised 22 July 2024; accepted 25 July 2024)

Abstract

A high-energy pulsed vacuum ultraviolet (VUV) solid-state laser at 177 nm with high peak power by the sixth harmonic of a neodymium-doped yttrium aluminum garnet (Nd:YAG) amplifier in a $KBe_2BO_3F_2$ prism-coupled device was demonstrated. The ultraviolet (UV) pump laser is a 352 ps pulsed, spatial top-hat super-Gaussian beam at 355 nm. A high energy of a 7.12 mJ VUV laser at 177 nm is obtained with a pulse width of 255 ps, indicating a peak power of 28 MW, and the conversion efficiency is 9.42% from 355 to 177 nm. The measured results fitted well with the theoretical prediction. It is the highest pulse energy and highest peak power ever reported in the VUV range for any solid-state lasers. The high-energy, high-peak-power, and high-spatial-uniformity VUV laser is of great interest for ultra-fine machining and particle-size measurements using UV in-line Fraunhofer holography diagnostics.

Keywords: high pulse energy; $KBe_2BO_3F_2$ prism-coupled device; spatial super-Gaussian beam; vacuum ultraviolet

1. Introduction

Deep ultraviolet (DUV) lasers (wavelength in the region of 190–250 nm) and vacuum ultraviolet (VUV) lasers (wavelength less than 190 nm)[1] have been in great demand for many applications, such as high-resolution photoemission spectroscopy, micromachining and photolithography[2–4]. There are various techniques to produce VUV sources, such as excimer lasers, free electron lasers (FELs), gas lasers and all solid-state lasers. All solid-state VUV lasers generated through second harmonic generation (SHG) or sum-frequency generation (SFG) have great application value and markets due to their longer lifetime and lower system maintenance cost. The shortest wavelength of 149.8 nm has been obtained by SFG in $KBe_2BO_3F_2$ (KBBF) by using the fundamental with its fourth harmonic of a Ti:sapphire laser[5]. However, during the SFG process, two laser beams are required to be precisely synchronized in both time and space, leading to a complex structure and low efficiency. Obtaining DUV or VUV laser by SHG from a diode-pumped solid-state laser (DUV/VUV-DPL) shows great application merits due to its compactness, high reliability and high conversion efficiency.

So far, the KBBF crystal is a unique crystal for the direct SHG approach to produce VUV coherent radiation effectively. Its transmittance cut-off wavelength is near 150 nm, and based on the improved Sellmeier equations, the minimum SHG wavelength is about 161 nm[6,7]. Since the KBBF crystal presents a plate-like architecture and is difficult to grow thick[8], a KBBF prism-coupled device (KBBF-PCD) was proposed to provide an important way for using the KBBF crystal perfectly to break the limitation of the phase-matching wavelength[9]. So far, based on the KBBF-PCD, a variety of DUV/VUV lasers have been reported[5,10–12]. In particular, sub-nanosecond (pulse

Correspondence to: N. Zong and L.-J. Liu, Technical Institute of Physics and Chemistry, Chinese Academy of Sciences, Beijing 100190, China. Emails: zongnan@mail.ipc.ac.cn (N. Zong); llj@mail.ipc.ac.cn (L.-J. Liu)

duration at hundreds of picoseconds) VUV pulse beams with high pulse energy, high peak power and high uniformity have the potential for ultra-fine machining and high-speed particle field measurements[13–16]. For example, for determining ejecta particle-size distributions, a high-resolution ultraviolet (UV) in-line Fraunhofer holography diagnostic is necessary. One important improvement of the measurement technique is to shorten the laser wavelength from 355 to 177 nm. Besides, the spatial super-Gaussian beam (SGB) with the pulse width of sub-nanosecond can insure a homogeneous illumination of the sample and capture the movement of the fastest ejecta without any motion blur[17].

Up to now, several VUV-DPLs with high energy, short pulse duration and high peak power have been reported. For nanosecond (ns) VUV-DPLs, a 0.375 mJ VUV laser at 177 nm was achieved from the sixth harmonic generation of a 1064 nm laser with the pulse width of 10 ns by a KBBF-PCD. This was the reported highest output energy previously for solid-state VUV lasers[18]. However, the corresponding peak power was only 0.1 MW. For picosecond (ps) VUV-DPLs, a pulse energy of 67 μJ at 177 nm was produced with a pulse repetition rate (PRR) of 10 Hz and a pulse duration of 20 ps. The SHG conversion efficiency from a UV to a VUV light source was nearly 10% and the peak power was 3.36 MW[19]. This result presents the highest conversion efficiency for VUV-DPLs. For VUV-DPLs with wavelengths less than 170 nm, due to low conversion efficiency and severe absorption loss in the KBBF crystal, the pulse energy was limited to the μJ level. For example, based on the eighth harmonic generation (EHG) of a 1319 nm laser, a 2.14 μJ ns VUV laser at 165 nm was obtained[20]. A single-frequency VUV laser at 167.079 nm with the pulse energy of 1.5 μJ by the EHG of a diode-pumped 1336.63 nm Nd:$(Lu_xGd_{1-x})_3Ga_5O_{12}$ (Nd:LGGG) laser was achieved[21].

In this paper, we developed a sub-nanosecond, spatial top-hat SGB VUV laser with high energy and high peak power by sixth harmonic generation of a 1064 nm neodymium-doped yttrium aluminum garnet (Nd:YAG) amplifier with two lithium triborate (LBO) crystals for the third harmonic generation (THG) and one KBBF crystal for the SHG. The highest pulse energy of 7.12 mJ at 177 nm with pulse duration of 255 ps was demonstrated, and the high peak power was up to 28 MW. By improving utilization of the pump laser and reducing the risk of KBBF-PCD damage under the high-energy pump laser with a narrow pulse width and spatial super-Gaussian (SG) profile, the VUV energy is about 18 times higher than the previous highest record. As far as we know, this VUV laser possesses both the highest pulse energy and highest peak power for any solid-state VUV laser that has been reported yet. In our work, the highest optical-to-optical (o-o) efficiency from 355 to 177 nm was up to 10%, which is the highest reported record from a UV to a VUV light source.

2. Experimental setup

Figure 1 shows the experimental configuration scheme from 1064 to 177 nm. Firstly, a 355 nm UV pulse was produced from a frequency tripled sub-nanosecond Nd:YAG master oscillator power amplifier (MOPA) at 1064 nm in two LBO crystals. A diode-pumped Nd:YAG passively *Q*-switched microchip laser at 1064 nm was used as the seed source. Then, the pulse energy of the seed source was amplified from 0.4 mJ to 1 J by a double-passing pre-amplifier and two single-passing side-pumped Nd:YAG main amplifiers. With three soft apertures in the amplification stages, a high-energy SGB with an approximately flat-top spatial profile at 1064 nm was obtained. The beam diameter and pulse width

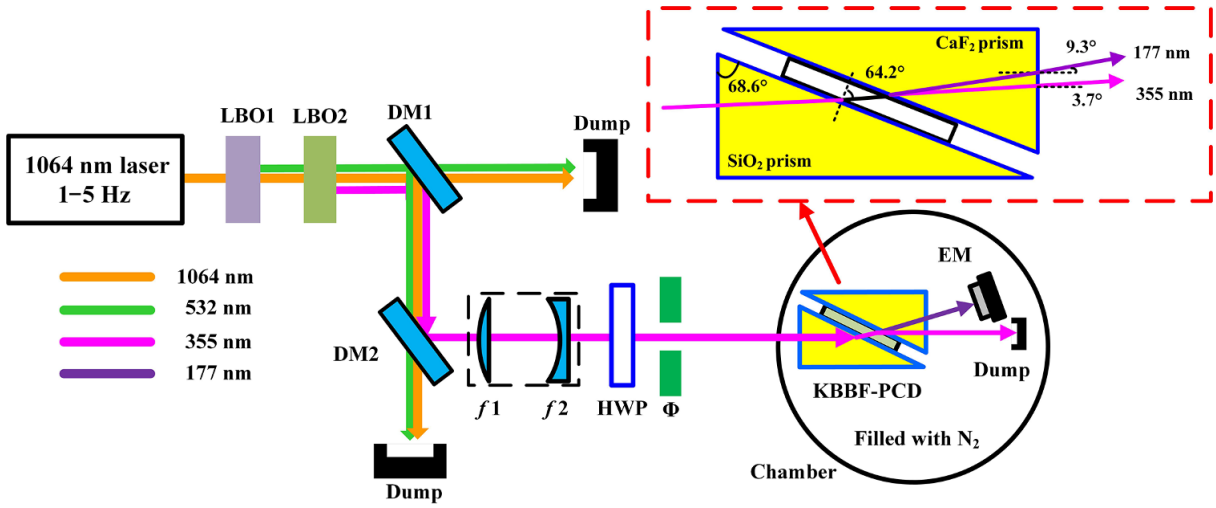

Figure 1. Schematic diagram of the high-energy sub-nanosecond VUV laser at 177 nm. Inset: detailed schematic structure of the KBBF-PCD in our experiment.

https://doi.org/10.1017/hpl.2024.46 Published online by Cambridge University Press

were 11 mm (D4σ) and approximately 400 ps (full width at half maximum (FWHM)), respectively, at the PRR of 1–5 Hz. A beam of 1064 nm was collimated approximately into a type-I noncritical phase-matched LBO1 crystal cut at $\theta = 90°$ and $\varphi = 0°$ with the dimensions of 14 mm × 14 mm × 10 mm operating at 148°C to produce the 532 nm second harmonic (SH) wave, which has wide acceptance angles and no walk-off effect. Both the end facets of the LBO1 crystal were antireflection (AR) coated for both fundamental and SH waves. At an input peak fundamental intensity of 1.1 J/cm^2, the highest output energy at 532 nm (measured by Coherent, J-50MB-AYG) was 748 mJ with a conversion efficiency of 74.5% from 1064 to 532 nm. The generated beam at 532 nm and the residual beam at 1064 nm were mixed in a type-II phase-matched LBO2 crystal cut at $\theta = 44.6°$ and $\varphi = 90°$ with the same size as the LBO1 crystal operating at 60.2°C to perform the THG at 355 nm. To avoid potential optical damage, only the LBO2 entrance facet was AR-coated for 1064 and 532 nm. At the input intensities of approximately 1.8 and 1 GW/cm^2 at 532 and 1064 nm, respectively, the highest energy at 355 nm was measured to be 428 mJ with the conversion efficiency of 43% from 1 μm to 355 nm[22].

Subsequently, the 355 nm UV beam was separated from residual 1064 and 532 nm beams by two dichroic mirrors, DM1 and DM2, and propagated toward the KBBF-PCD for the SHG. To obtain high conversion efficiency and stay above the damage threshold of the devices from the high-peak-power laser, a 2:1 beam shaping system (f_1+f_2) collimated the 355 nm pump beam to a diameter of 5.5 mm, which corresponds to the available crystal aperture of 16 mm × 6 mm in our lab. A half-wave plate (HWP) was employed to adjust the polarization of the 355 nm beam along the x-axis of the KBBF crystal. Then, to reduce the influence of diffraction on the KBBF-PCD, the 355 nm beam going through a hard aperture was injected into the KBBF-PCD to achieve a sixth harmonic at 177 nm. The energy of the 177 nm pulse was measured by a pyroelectric energy meter (OPHIR, PE10-C, 0.15–12 μm, 1 μJ–10 mJ). Due to the strong absorption of DUV/VUV light in air, VUV components were placed in a N_2-filled chamber, as shown in Figure 1.

For the KBBF-PCD, by optical contact the KBBF crystal was sandwiched between a SiO_2 prism and a CaF_2 prism having apex angles of 68.6° with the size of 9 mm × 23 mm × 9 mm, as shown in the inset of Figure 1. The SiO_2 prism with a high laser damage threshold was used as the front prism and CaF_2 was employed as the rear prism because of its relatively low absorption coefficient for the VUV laser. Based on the Sellmeier equation of KBBF crystal as follows[7]:

$$n_o^2 = 1.024248 + \frac{0.9502782\lambda^2}{\lambda^2 - 0.0738546} + \frac{0.1960298\lambda^2}{\lambda^2 - 0.1298386^2} - 0.0113908\lambda^2, \quad (1)$$

$$n_e^2 = 0.9411543 + \frac{0.8684699\lambda^2}{\lambda^2 - 0.0646955^2} + \frac{0.1256642\lambda^2}{\lambda^2 - 0.1196215^2} - 0.0044736\lambda^2, \quad (2)$$

the phase-matching angle from 355 to 177 nm in the KBBF crystal is calculated to be 64.2°. Here, the KBBF-PCD was fixed into a metal holder and blown by the N_2 flow, which is also helpful for removing the heat away from the crystal. The KBBF-PCD was equipped with a high-precision rotator. Therefore, the angle of incidence on the KBBF-PCD can be changed precisely to achieve a 177 nm laser efficiently.

3. Theoretical analysis

As is well known, to obtain high-efficiency VUV light generation, the length of the nonlinear crystal should be analyzed emphatically. For the KBBF-SHG process in the sub-nanosecond regime, the group-velocity mismatch (GVM; 600.6 fs/mm) and group-velocity dispersions (GVDs) (102.9 fs^2/mm@355 nm, 286 fs^2/mm@177 nm) of the wave fields can be neglected. Considering pump depletion, diffraction, spatial birefringent walk-off and the losses from the crystal and coupled prism, the coupled-wave equations explaining the propagation of sub-nanosecond lasers along the longitudinal coordinate z during the SHG process present the following expressions[23]:

$$\frac{\partial A_1(x,y,z,t)}{\partial z} = \frac{j}{2k_1}\left(\frac{\partial^2}{\partial x^2} + \frac{\partial^2}{\partial y^2}\right)A_1(x,y,z,t) - \frac{\alpha_1}{2}A_1(x,y,z,t) + j\sigma_1 A_2 A_1^* \exp(i\Delta k z), \quad (3)$$

$$\frac{\partial A_2(x,y,z,t)}{\partial z} = \frac{j}{2k_2}\left(\frac{\partial^2}{\partial x^2} + \frac{\partial^2}{\partial y^2}\right)A_2(x,y,z,t) - \tan\rho\frac{\partial A_2(x,y,z,t)}{\partial x} - \frac{\alpha_2}{2}A_2(x,y,z,t) + j\sigma_2 A_1^2 \exp(-i\Delta k z), \quad (4)$$

where A_1 and A_2 are the complex amplitudes of the 355 nm pump beam and the VUV beam, respectively; ρ is the spatial walk-off angle; and α_1 and α_2 are linear absorption coefficients at the pump wave and SH wave, respectively. Here, $\sigma_i = \omega_1 d_{\text{eff}}/n_i c$ (i = 1, 2) is the second-order nonlinear coupling coefficient and $\triangle k = 2k_1 – k_2$ is the wave vector mismatch, where ω_1 is the angular frequency of the 355 nm pump wave; d_{eff} is the effective nonlinear coefficient of the KBBF crystal; n_1 and n_2 are the refractive indices of the pump beam and VUV beam in the KBBF crystal, respectively; and c is the speed of light in vacuum. While the spatial and temporal profiles of the pump laser are supposed to be SG shaped and Gaussian shaped, respectively, and the pump beam Rayleigh distance is much larger than the crystal

https://doi.org/10.1017/hpl.2024.46 Published online by Cambridge University Press

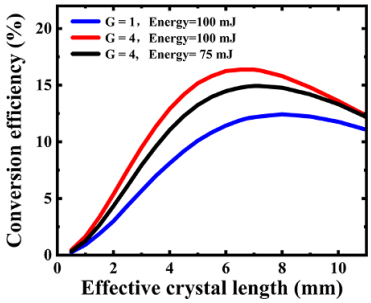

Figure 2. Calculated conversion efficiency from 355 to 177 nm versus KBBF effective crystal length for Gaussian beam $G = 1$ and SGB $G = 4$ at the pump energies of 100 and 75 mJ with a beam diameter of 5 mm.

length, the complex amplitude of the pump laser could be shown as follows[23,24]:

$$A(x,y,z,t) = \frac{A_0}{w_0}\exp\left[-\left(\frac{x^2+y^2}{w_0^2}\right)^G\right]\exp\left(-\frac{t^2}{\tau^2}\right), \quad (5)$$

where A_0 is the center amplitude; w_0 is the radius of the SGB; τ is half the pulse width ($1/e^2$); and G is an integer indicating the order of the SGB. For the usual Gaussian beam, G is 1. As the value of G increases, the closer the SGB approximates a true spatial top-hat beam. In our work, based on the measured filling factor of 0.428 at 355 nm, the order of G is about 4[25]. Based on the fourth-order Runge–Kutta method, the above equations can be integrated numerically. Then, the output characteristics of the VUV laser can be obtained. The parameters used in our numerical model are $\tau = 300$ ps, $\rho = 65.40$ mrad, $d_{\text{eff}} = 0.287$ pm/V, $\triangle k = 0$, $\alpha_1 = 0.1$ cm^{-1} and $\alpha_2 = 1.2$ cm^{-1}[7,26]. The absorption loss of 177 nm light in a CaF_2 prism (0.2 cm^{-1}) is considered in numerical calculations.

Due to the limited aperture of the KBBF crystal of 16 mm × 6 mm, the maximum normally incident light spot diameter in the SiO_2 prism is 5.838 mm. To reduce the influence of diffraction on the KBBF-PCD, a hard aperture was used to limit the diameter of the 355 nm beam to 5 mm. Figure 2 shows the calculated conversion efficiency under different crystal lengths for the Gaussian beam and SGB with $G = 4$ under pump energies of 100 and 75 mJ with an input spot diameter of 5 mm. It can be seen that SHG conversion efficiency could be significantly raised by increasing the uniformity of the pump beam. For $G = 4$, we can see that the maximum conversion efficiency of 16.3% under pump energy of 100 mJ is obtained by extending the effective crystal length to approximately 6 mm, and then it starts to drop for a longer crystal due to the absorption loss and the spatial walk-off effect in the KBBF crystal. Under the pump energy of 75 mJ, the optimal effective crystal length is 6.8 mm, corresponding to the maximum conversion efficiency of 14.9%. A 1.7 mm thick KBBF crystal with effective crystal length of 4 mm was employed in the following investigation, corresponding to the calculated conversion efficiencies of 13% and 11% at pump energies of 100 and 75 mJ, respectively.

4. Results and discussion

Figure 3 shows the VUV laser output performance at the PRRs of 3 and 5 Hz. The circles and triangles show the measured data of energy and conversion efficiency, and the calculated results are shown as well. For a given 355 nm pump energy, the output energy at 177 nm decreases with the increase of the PRR. At the PRR of 3 Hz, the highest output energy of 7.12 mJ was achieved at the input energy of 75.6 mJ by a KBBF-PCD with an SHG conversion efficiency of 9.42%. This VUV laser energy is about 18 times more than the previous record by Wen *et al.*[18]. KBBF crystals have a high damage threshold of 60 GW/cm^2 (390 nm, 200 fs, 1 kHz)[8]. However, the damage threshold of the KBBF-PCD is limited by the optical contact surface. Based on previous research work, the damage threshold of the KBBF-PCD is over 1.2 GW/cm^2 (10 Hz, 30 ps, 355 nm)[19]. To prevent KBBF-PCD damage during the experiment, there is no further increase in the input energy. The conversion efficiency displays a saturation behavior. At the input energy of 41.6 mJ, the single pulse energy at 177 nm was 4.17 mJ, resulting in a maximum conversion efficiency of approximately 10%, which has reached the highest conversion efficiency reported from 355 to 177 nm[19]. At the PRR of 5 Hz, at an input energy of 72.8 mJ at 355 nm, 6.33 mJ 177 nm output is obtained, and the corresponding conversion efficiency is 8.7%. The calculated output energy is also displayed in Figure 3 with a black line. It is observed that the measured data fit well with the simulated results for the pump energy of less than 50 mJ. With the input energy further increasing, the calculated results were slightly higher than the experimental values. In particular, the measured results at 5 Hz deviate more from the theoretical simulation than that at 3 Hz due to more serious thermal effects at higher PRRs. The deviation could mainly come from not taking into account the thermal effect in the theoretical model, which may lead to phase-mismatching, and that decreases the output energy.

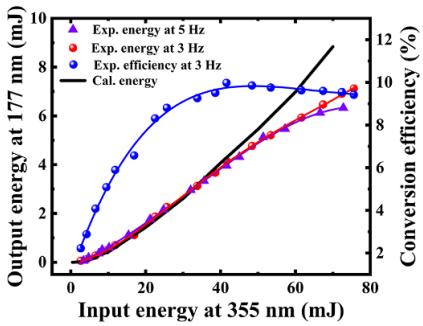

Figure 3. Dependence of output energy of the 177 nm laser and conversion efficiency of the pump energy at 355 nm.

https://doi.org/10.1017/hpl.2024.46 Published online by Cambridge University Press

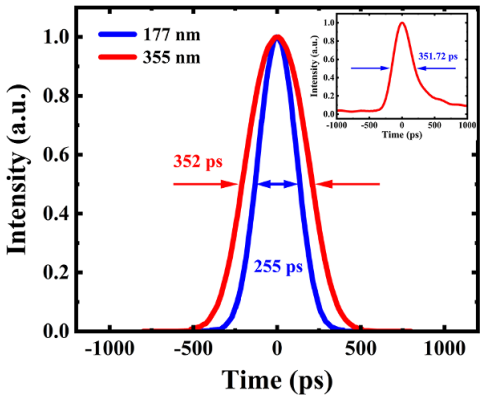

Figure 4. Simulated 355 and 177 nm pulse temporal profiles. Inset: measured pulse profile of the 355 nm laser.

So far, after six months, the KBBF crystal and the prisms of the PCD are all intact.

Due to the lack of a suitable detector for sub-nanosecond VUV lasers in our lab, we measured the pulse width of 355 nm, and then simulated the pulse duration of 177 nm beam after the KBBF crystal by solving Equations (3)–(5). The temporal characteristic of the pump laser at 355 nm was collected by a high-speed detector (ALPHALAS GMBH, UPD-40-UVIR-P, rise time <40 ps, bandwidth >7.5 GHz, 350–1700 nm) and recorded on a phosphor digital oscilloscope (Keysight MSOS404A, 4 GHz bandwidth, rise time <107.5 ps). A typical pulse profile at 3 Hz is shown in the inset of Figure 4 at the full output pulse energy, recorded pulse width of $\tau_i = 351.72$ ps (FWHM), with measured error of about 16% or 56 ps from the response of the detector and the oscilloscope. Therefore, the measured pulse width of 355 nm is 352 ± 56 ps. Assuming the 355 nm pump pulse with a Gaussian temporal profile, the calculated SHG temporal profile at 177 nm became narrow and the pulse duration of the 177 nm pulse was about 255 ps, as shown in Figure 4. It can be noticed that the pulse duration at 177 nm is approximately $\tau_i/\sqrt{2}$ owing to the SHG temporal gain narrowing effect in homogeneous materials[27]. Consequently, the highest peak power of VUV lasers can reach 28 MW.

At the maximum output energy, the spectrum of the input pulse was obtained by a spectrometer (Avantes, AvsSpec-ULS4096CL-EVO, resolution 0.5–0.7 nm, 200–1100 nm), as shown in Figure 5(a), recorded at 354.8 nm. The measured center wavelength of the pump UV laser locates at 354.9 ± 0.1 nm. Thus, the corresponding SH VUV wavelength is obtained as 177.45 ± 0.05 nm. Figure 5(b) illustrates the near-field two-dimensional (2D) beam spatial profile at 355 nm, recorded using a laser beam profiler (Ophir, Spiricon, SP932U USB 2048×1536 CMOS, 190–1100 nm). We can see that the pump spot profile is similar to a round top-hat spatial shape. To confirm whether the sixth harmonic was generated, a fluorescence glass plate was used to display the fluorescence patterns induced by the residual beam at 355 nm and the generated beam at 177 nm, respectively, as shown in Figure 6.

5. Conclusion

In summary, we have succeeded in obtaining a high-energy, high-peak-power, sub-nanosecond, high-uniformity VUV laser by the sixth harmonic generation of a 1064 nm Nd:YAG MOPA system. A new record-high output energy of 7.12 mJ at 177 nm was generated from a KBBF-PCD while the pump energy at 355 nm was 75.6 mJ, resulting in a conversion efficiency of 9.42% from a UV to a VUV light source. The calculated results agree well with the experimental data. Moreover, the pulse duration of the generated 177 nm radiation was analyzed to be 255 ps and the peak power was approximately 28 MW. As far as we know, these results demonstrate both the highest pulse energy and the highest

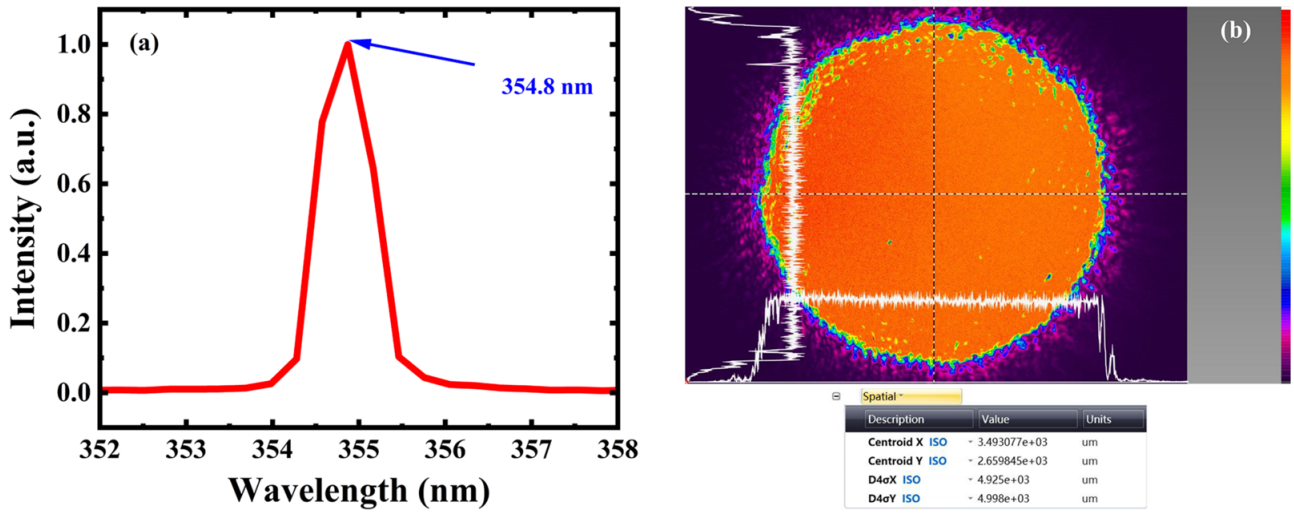

Figure 5. Measured spectrum of the pump laser and near-field 2D beam spatial profile at 355 nm.

https://doi.org/10.1017/hpl.2024.46 Published online by Cambridge University Press

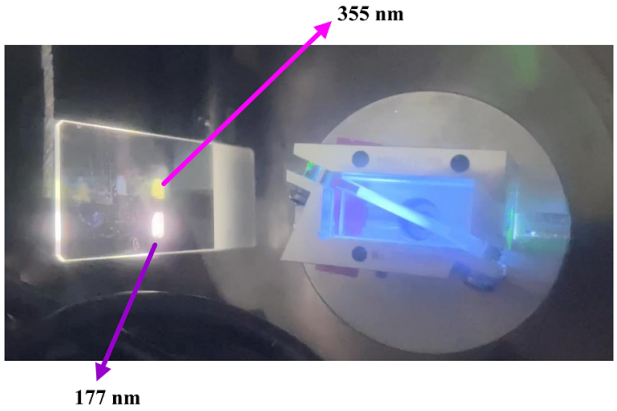

Figure 6. Fluorescence patterns on the fluorescence glass induced by the residual beam at 355 nm and the generated beam at 177 nm.

peak power for any VUV solid-state laser. By enlarging the KBBF crystal aperture (the largest aperture is 30 mm × 10 mm now), increasing the pump energy, enhancing the damage threshold of the KBBF-PCD by improving the processing technology and controlling the temperature of the KBBF crystal, further scaling into the range of several tens of mJ pulse energy is possible. This high-energy, high-peak-power, sub-nanosecond VUV light source with a spatial top-hat beam has great potential application prospects in ultra-fine machining and precise measurements of high-speed particle fields using UV in-line Fraunhofer holography diagnostics.

Acknowledgements

This work was supported by the National Key Research and Development Program of China (No. 2023YFB3610601), the International Partnership Program for Grand Challenges of the Chinese Academy of Sciences (No. 174GJHZ2022016GC) and the National Special Program for High-level Talents Science and Technology (No. SQ2022RA24910010)

References

1. P. Misra and M. A. Dubinski, *Ultraviolet Spectroscopy and UV Lasers*, Practical Spectroscopy Series (Marcel Dekker, Inc., New York, 2002), p. 16.
2. L. von der Wense, B. Seiferle, S. Stellmer, J. Weitenberg, G. Kazakov, A. Palffy, and P. G. Thirolf, Phys. Rev. Lett. **119**, 132503 (2017).
3. A. Ozawa, J. Davila-Rodriguez, J. R. Bounds, H. A. Schuessler, T. W. Hansch, and T. Udem, Nat. Commun. **8**, 44 (2017).
4. G. Liu, G. Wang, Y. Zhu, H. Zhang, G. Zhang, X. Wang, Y. Zhou, W. Zhang, H. Liu, L. Zhao, J. Meng, X. Dong, C. Chen, Z. Xu, and X. Zhou, Rev. Sci. Instrum. **79**, 023105 (2008).
5. T. Nakazato, I. Ito, Y. Kobayashi, X. Wang, C. Chen, and S. Watanabe, Opt. Express **24**, 17149 (2016).
6. C. Chen, G. Wang, X. Wang, Y. Zhu, Z. Xu, T. Kanai, and S. Watanabe, IEEE J. Quantum Elect. **44**, 617 (2008).
7. R. Li, L. Wang, X. Wang, G. Wang, and C. Chen, Appl. Opt. **55**, 10423 (2016).
8. C. T. Chen, G. L. Wang, X. Y. Wang, and Z. Y. Xu, Appl. Phys. B **97**, 9 (2009).
9. C. Chen, Z. Xu, J. Lv, and G. Wang, "Prism-nonlinear optical crystal coupler for laser frequency conversion". U.S. patent, US 6859305 B2 (Februray 22, 2005).
10. T. Kanai, X. Wang, S. Adachi, S. Watanabe, and C. Chen, Opt. Express **17**, 8696 (2009).
11. X. Zhang, Z. Wang, G. Wang, Y. Zhu, Z. Xu, and C. Chen, Opt. Lett. **34**, 1342 (2009).
12. S. B. Dai, N. Zong, F. Yang, S. J. Zhang, Z. M. Wang, F. F. Zhang, W. Tu, L. Q. Shang, L. J. Liu, X. Y. Wang, J. Y. Zhang, D. F. Cui, Q. J. Peng, R. K. Li, C. T. Chen, and Z. Y. Xu, Opt. Lett. **40**, 3268 (2015).
13. I. Giuntoni, D. Stolarek, H. Richter, S. Marschmeyer, J. Bauer, A. Gajda, J. Bruns, B. Tillack, K. Petermann, and L. Zimmermann, IEEE Photonic. Tech. Lett. **21**, 1894 (2009).
14. A. Bonakdar, M. Rezaei, R. L. Brown, V. Fathipour, E. Dexheimer, S. J. Jang, and H. Mohseni, Opt. Lett. **40**, 2537 (2015).
15. D. Sorensona, R. Maloneb, B. Froggetb, C. Ciarciab, T. Tunnellb, and R. Flurer, in *22nd International Congress on High-Speed Photography and Photonics* (1996), p. 206.
16. D. Sorenson, G. Capelle, M. Grover, R. Johnson, M. Kaufman, B. LaLone, R. Malone, B. Marshall, R. Minich, P. Pazuchanics, D. Smalley, G. Stevens, T. Tunnell, and W. Turley, J. Dynam. Behav. Mat. **3**, 233 (2017).
17. A. Sollier and E. Lescoute, Int. J. Impact Eng. **136**, 103429 (2019).
18. N. Wen, N. Zong, F. F. Zhang, F. Yang, Z. M. Wang, S. J. Zhang, Y. Bo, Q. J. Peng, D. F. Cui, Z. Y. Xu, X. Y. Wang, L. J. Liu, and R. K. Li, Laser Phys. Lett. **17**, 105001 (2020).
19. C. Li, Y. Zhou, N. Zong, Z. Xu, X. Wang, and Y. Zhu, Chin. Opt. Lett. **7**, 621 (2009).
20. S. B. Dai, M. Chen, S. J. Zhang, Z. M. Wang, F. F. Zhang, F. Yang, Z. C. Wang, N. Zong, L. J. Liu, X. Y. Wang, J. Y. Zhang, Y. Bo, D. F. Cui, Q. J. Peng, R. K. Li, C. T. Chen, and Z. Y. Xu, Laser Phys. Lett. **13**, 035401 (2016).
21. J. J. Li, F. F. Zhang, Z. M. Wang, Y. C. Xu, X. C. Liu, N. Zong, S. J. Zhang, F. L. Xu, F. Yang, L. Yuan, Y. Kou, Y. Bo, D. F. Cui, Q. J. Peng, X. Y. Wang, L. J. Liu, C. T. Chen, and Z. Y. Xu, Opt. Lett. **43**, 2563 (2018).
22. N. Wang, J. Zhang, H. Yu, X. Lin, and G. Yang, Opt. Express **30**, 5700 (2022).
23. Z. Xu, F. Zhang, S. Zhang, Z. Wang, F. Yang, F. Xu, Q. Peng, D. Cui, J. Zhang, X. Wang, C. Chen, and Z. Xu, Laser Phys. **24**, 065401 (2014).
24. S. Silvestri, P. Laporta, V. Magni, O. Svelto, and B. Majocchi, Opt. Lett. **13**, 201 (1988).
25. W. W. Simmons, J. T. Hunt, and E. W. Williame, IEEE J. Quantum Electron. **17**, 1727 (1981).
26. C. Xu, S. Dai, C. Guo, Q. Bian, J. Zuo, Y. Xia, H. Gao, M. Wang, Y. Bo, N. Zong, S. Zhang, Q. Peng, and Z. Xu, Chin. Phys. Lett. **34**, 034206 (2017).
27. R. W. Boyd, *Nonlinear Optics*, 3rd Ed. (Elsevier Academic Press Inc., New York, 2003).

https://doi.org/10.1017/hpl.2024.46 Published online by Cambridge University Press